Computers and Electronics in Agriculture 127 (2016) 271–280

Contents lists available at ScienceDirect

Computers and Electronics in Agriculture

journal homepage: www.elsevier.com/locate/compag

Spatial behavioral characteristics and statistics-based kinetic energy modeling in special behaviors detection of a shoal of fish in a recirculating aquaculture system

Jian Zhao [a], Zhaobin Gu [b], Mingming Shi [a], Huanda Lu [c], Jianping Li [a], Mingwei Shen [a], Zhangying Ye [a,*], Songming Zhu [a,*]

[a] School of Biosystems Engineering and Food Science, Zhejiang University, Hangzhou 310058, PR China
[b] College of Animal Science Technology, Yunnan Agricultural University, Kunming 650201, PR China
[c] Ningbo Institute of Technology, Zhejiang University, Ningbo 315100, PR China

ARTICLE INFO

Article history:
Received 21 August 2015
Received in revised form 20 June 2016
Accepted 21 June 2016
Available online 27 June 2016

Keywords:
Fish welfare
RAS
Modified kinetic energy model
Spatial behavioral characteristics
Dispersion status
Changing magnitude of the motion

ABSTRACT

In global aquaculture, fish welfare is attached increasing importance to. Fish behavior holds important information of its living welfare. Thus, in order to detect special behaviors concerned with fish welfare in a recirculating aquaculture system (RAS), a modified kinetic energy model of the whole shoal instead tracking individuals inside a shoal was proposed in this study. The dispersion, velocity and turning angle of the shoal were regarded as the key factors in this model. First, with the reflective regions of the water surface taken into account, two alternative ways were presented to extract the necessary spatial behavioral characteristics of the shoal. Then, optical flow, entropy and statistics were adopted to measure the dispersion status (dispersion of individuals in space) and the changing magnitude of the motion (behavioral characteristics) of the shoal. Finally, the modified kinetic energy model was obtained by combining the dispersion measurement with the changing magnitude of the behavioral characteristics. Referring to the human observation and the evacuation of the gastro-intestine contents-based long experiment of Nile tilapia (*Oreochromis niloticus*) in RAS, the proposed model shows good performance in detection of the emergent gathering and scattering behaviors with 97.20 ± 1.23% success rate at least and 0.61 ± 0.08% missing report rate at most.

1. Introduction

Nowadays fish welfare is emphasized in aquaculture, and the physiological and mental states of fish are studied with relation to their living environment (Polten, 2007; Kiessling et al., 2012; Jones, 2013). Most physiological, mental and environmental changes are capable of inducing variations in fish behavior. In other words, fish behavior holds important information of the living quality (Masud et al., 2005; Pratt et al., 2005; Miller and Gerlai, 2007; Mancera et al., 2008). Furthermore, in view of increasing scarcity of global water resource, the industrial recirculating aquaculture system (RAS) is becoming the trend of aquaculture although most production take place in land-based at present. RAS has the ability of maintaining good rearing conditions for the optimized growth and feed utilization of a given species (Le François et al., 2010). They are all necessary prerequisites for the sustainable development of aquaculture (Dalsgaard et al., 2013). Thus, the behavioral research of the fish in RAS may show the best prospect.

Due to the sensitivity of the fish to the changes of the living environmental parameters, the methods through continuously monitoring and quantifying behavioral response of fish are potential measurements for assessing fish living states (Vassilis et al., 2012). In fish farming systems, the earlier detection of special behaviors, the less loss of the fish production.

Traditional video recording has the ability of the remote observation of the fish behavior in real time, and also for the offline reproduction of fish activity through video playback (Vogl et al., 1999). The major advantage of video systems is the fact that no human presence is required to observe the fish behavior in aquaculture workshop. Nevertheless, generally speaking, traditional analysis of the recorded video is very hard to be performed due to the fact that the long duration of the recorded video is, the equal

* Corresponding authors at: Zhejiang University, 866 Yuhangtang Rd., Hangzhou, Zhejiang 310058, PR China.
E-mail address: yzyzju@zju.edu.cn (Z. Ye).

http://dx.doi.org/10.1016/j.compag.2016.06.025
0168-1699/

or more consumption of the time spent for observation from a person would be.

Computer vision techniques provide an automated, non-invasive and cost-effective method for remote behavioral analysis of the fish in real time. To date, some research has been conducted on this aspect at laboratory scale. Most of these studies placed emphasis on observing the physical statuses of the fish or environmental variations by monitoring the behavioral changes of individual fish. Hypoxic conditions (Xu et al., 2006), stress responses (Kane et al., 2004; Papadakis et al., 2012), motion responses (Gui et al., 2006), vertical distributions (Stien et al., 2007), and genetic statuses (Robbert, 2009) by image analysis have been reported. These studies are based on tracking individual fish rather than tracking a shoal. Nevertheless, according to the previous research (Delcourt et al., 2009, 2013), the essence of computer vision techniques-based behavioral analysis of the shoal is the tracking of the individuals through location technology. The quality of tracking determines the results of the behavioral analysis. Whereas, multi-target tracking in a group is still a challenge in computer science. Thus, tracking individual fish among a shoal is difficult to be implemented, especially in intensive industrial RAS. Furthermore, according to Campenhausen et al. (1981) and Conrad et al. (2011), contrasted to the behavior of individual fish, special behaviors of the whole shoal especially the emergent gathering and scattering may indicate huger information about particular events such as feeding, defense, conflict and stress.

Kinetic energy model can be used to express the motion status of the objects by making use of the necessary motion features. At present, few works using kinetic energy on fish have been reported. Most studies on kinetic energy are focused on the abnormal events detection of the crowd. Earlier, Zhong et al. (2007) defined the kinetic energy model with the consideration of only the crowd velocity. Cao et al. (2009) improved the kinetic energy model by adopting the crowd ratio parameter of the foreground area to the background area. Recently, Guo et al. (2012) modified the kinetic energy model by calculating the dispersion information through defining crowd entropy to represent the spatial distribution of the foreground crowd. However, all kinetic energy models mentioned above depended on the necessary foreground segmentation, and only the information of the dispersion and velocity was took into account, the impact of the turning angle or direction was ignored.

Velocity is an important reference factor in measurement of the status of the fish. Wyatt (1972) reported that the flatfish in starved conditions shows faster velocity and motion level than flatfish in no-starvation conditions. Liu et al. (2014) made use of the moving velocity of the shoal to measure the feeding activity by means of the computer vision. The moving velocity was also treated as the necessary representation of the stress response of the fish (Kane et al., 2004; Xu et al., 2006; Papadakis et al., 2012). Due to the randomness of the fish in space-time, not only the velocity but also the turning angle of the fish should be attached importance to. In addition, to some extent, the dispersion of the shoal also indicates the status of the shoal (Israeli and Kimmel, 1996; Xu et al., 2006; Stien et al., 2007; Conrad et al., 2011). Thus, the necessary information of the velocity, turning angle and dispersion was taken into account to express the spatial behavioral characteristics of the shoal in this study. For this purpose, a novel modified kinetic energy model (KEM) for the whole shoal instead tracking of individuals was proposed to detect special behaviors of the shoal in RAS.

First, the spatial behavioral characteristics were extracted in two different ways: 1. Improved average background modeling based foreground segmentation (BMFS); 2. Particle advection scheme and optical flow-based necessary particles extraction (PAOF) without the foreground segmentation but in consideration of the reflective regions of the water surface (the reflective regions was alleviated using Sobel filter since it is an algorithm which can be used to detect the edges of the targets). Secondly, the behavioral characteristics statistics and entropy-based measurement of the dispersion status of the shoal was obtained. Then, the changing magnitude of the behavioral characteristics was assessed through the calculation of the joint statistics of velocities and turning angles of the shoal. Finally, combined with the dispersion measurement and changing magnitude of the behavioral characteristics, the modified kinetic energy model was executed to detect the different special behaviors of the shoal.

In this study, Nile tilapia (*Oreochromis niloticus*) was regarded as the experimental objects as its indispensable status in Chinese agricultural economic system which makes China become the main country of the tilapia production worldwide. The purpose of this study was to build the potential and efficient method to detect and recognize the different special behaviors of the shoal and provide reliable theoretical support for on-line smart supervision in aquaculture, especially in RAS, to ensure the fish welfare.

2. Materials and methods

2.1. Fish

All tilapia were provided by a farm (North Supreme Seafood Co. Ltd., Zhejiang, China). They were first acclimated in the experimental RAS for 2 months. During the acclimation and experimental phases, the fish (60 tilapias with (60 ± 10) g in each RAS) were placed under a 12 h:12 h light-dark cycle (07:00–19:00 light, 19:00–07:00 dark) and fed 3 times a day (00:80, 12:00, and 16:00). The feeding amount per day was set to 5% of the body weight of the shoal.

2.2. Experimental system

2.2.1. RAS structure

The experimental RAS (Fig. 1) mainly consisted of a rearing tank (100 cm radius and 80 cm depth), solid removal component, biofilter, UV light source, skimmer, oxygen supply device and feeding machine. The feeding machine was set through Programmable Logistical Controller (PLC, FX2N, Mitsubishi). During the entire acclimation and experiment, the following conditions were maintained: dissolved oxygen (DO) at (6.5 ± 0.5) mg/L, total ammonia nitrogen (TAN) <0.6 mg/L, temperature at (27 ± 2) °C, pH at 7.8 ± 0.3, and chemical oxygen demand (COD) <1.5 mg/L.

2.2.2. Computer vision system

The computer vision system (Fig. 1) possessed a video capture subsystem (Dell Server: CPU Xeon X5650, 2.66 GHz, 24 GB memory; CCD HDV (camera): DS-2CD6233F-SDI, Hikvision) and an illumination subsystem with an LED (100 W, Kingbright). The HDV was installed facing downward toward the water surface (1.2 m from the water surface) over the center of the tank, and 24-bit RGB images were acquired with a resolution of 1080 × 1920 pixels. The frames were captured at a rate of 25 fps. The LED controlled by PLC was affixed to the top of the wall (2.7 m from the water surface). To obtain a relatively uniform light intensity and avoid the direct projection of light onto the water surface, soft fabric was placed around the LED.

2.2.3. Experimental procedure

According to Wyatt (1972), the hunger the shoal is, the more special and intense behaviors (such as feeding and stress behaviors) the shoal would make. Thus, in order to capture the spontaneous behaviors of the emergent gathering and scattering as many as possible, experiment in this study was based on the evac-

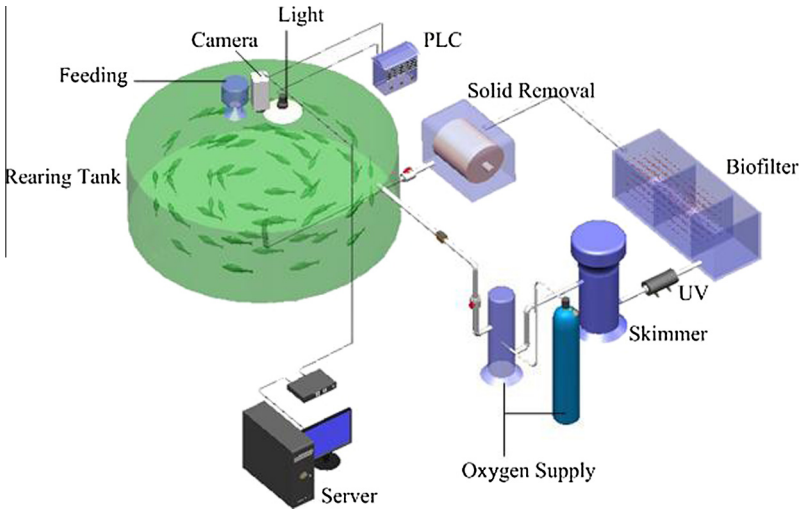

Fig. 1. The experimental RAS structure and video capture system.

uation of the gastro-intestine contents (Amundsen and Klemetsen, 1988). Before the experiment, fish were restricted from feeding for 36 h to ensure that minimal food remained in the stomach and intestine. During the experiment, fish in three experimental tanks were simultaneously fed to over-satiation first. Then, the fish in three experimental tanks were restricted from feeding for 36 h once again (in the meantime, the LED was turned on). The cameras which were installed over the experimental tanks recorded the activities of the shoal once the over-feeding was carried out. The above experiment was implemented at intervals of one week and for 4 cycles.

2.3. KEM-based detection of special behaviors of the shoal in RAS

2.3.1. Extraction of the spatial behavioral characteristics of the shoal

2.3.1.1. Determined by the BMFS-based method. In order to obtain the dispersion information of the shoal, the analysis directly focused on the distribution of the foreground may be an effective way.

Fig. 2 shows the processing procedure of foreground segmentation of the shoal. First, a test image was translated from an RGB color model (Fig. 2(A)) to a YCbCr color model (Fig. 2(B)), and the Cr component intensity image of the YCbCr (Fig. 2(C)) was extracted due to the background being lighter than the shoal in the Cr component compared with other components.

To adapt to the changing environment, the background model was updated dynamically with the help of an improved average background modeling method in the Cr component by weighing the fixed background frames (Eq. (1)).

$$B_t(x,y) = \alpha B(x,y) + \beta F_t(x,y) \tag{1}$$

where $B_t(x,y)$ is the background modeling at time t, $B(x,y)$ is the fixed background image due to the virtually unchanging tank background in real RAS, $F_t(x,y)$ is the aquaculture image at time t. α and β denotes the refresh rates of the background image and aquacul-

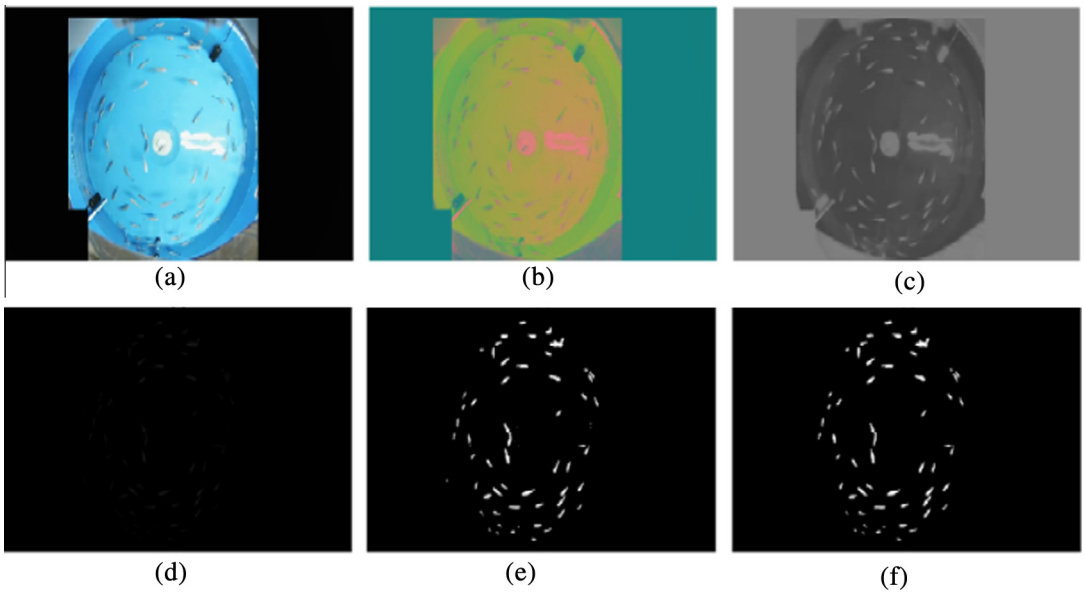

Fig. 2. (a) Typical experimental image in RGB, (b) typical experimental image in YCbCr, (c) typical experimental intensity image in the Cr component, (d) the resulting image of the background subtraction in the Cr component, (e) the binary result using OSTU method and (f) the foreground image after the operation of the morphology and Freeman 8-chain code.

ture image, respectively. To obtain a good result of the background updating, α and β were set to 0.5 and 0.5, respectively, via the amounts of experiments. Then the foreground of the shoal was obtained by Eq. (2).

$$F'_t(x,y) = |F_t(x,y) - B_t(x,y)| \quad (2)$$

where $F'_t(x,y)$ is the foreground of the shoal at time t (Fig. 2(D)).

Finally, the binary foreground of the shoal (regarded as the behavioral characteristics) was obtained by a self-adaptive square error analyzing method (OSTU, 1979) which can be used to determine the gray threshold of the foreground and background in an image (Fig. 2(E)). The morphological operation (Gonzalez and Woods, 2002) which can be used to dilate or erode the target and Freeman 8-chain code (Tang, 1982) which can be used to calculate the area of the target in eight directions, were adopted to reduce the disturbance caused by other objects, such as fragments of feed and bubbles, by removing the objects with areas less than a pixels (Fig. 2(F)). In this study, a was set to 50.

2.3.1.2. Determined by the PAOF-based method. Generally speaking, method in Section 2.3.1.1 may be applicable to the extraction of the behavioral characteristics of the shoal in an ideal RAS. Nevertheless, in real industrial RAS, the stable background for foreground segmentation of the shoal is difficult because of the disturbance of the complex environment such as water level, reflective regions of the water surface and equipments placed at the tank.

In recent years, in order to overcome the limitations of complex foreground segmentation in crowd scene, some researchers concentrate their attention on particle advection schemes (Ali and Shah, 2007) that a grid of particles were placed on frame to simulate individuals in the crowd and advected with the optical flow. Therefore, in this section, similar particle advection scheme was adopted to avoid the complex foreground segmentation. In the meantime, because of the usage of the optical flow, tracking of individuals was avoided.

The extraction of the behavioral characteristics of the shoal using optical flow was accomplished by calculating the motion characteristics, including the amplitudes (velocities) and directions (turning angles) of the corresponding pixels (Section 2.3.3). Fig. 3 is the example of optical flow (detailed in Section 3) through the calculation of the consecutive three frames in Cr component. To have an optimum visibility, the optical flow in Fig. 3 was calculated at intervals of 20 pixels.

It should be noted that water reflection caused by the intense behaviors of the shoal may disturb the dispersion measurement (Section 2.3.2). So, referring to Liu et al. (2014), a 5×5 Sobel filter (Sobel, 1990) was implemented to detect the edges of the reflective regions in an R intensity image since the reflective regions in R component is more distinct than that in the other components. The optical flow information including velocities and turning angles of the pixels in these regions were set to zero.

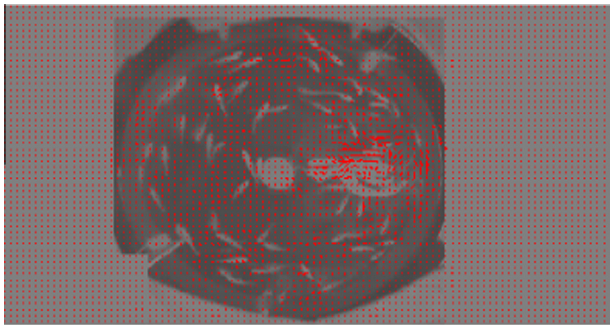

Fig. 3. Optical flow (red) of the shoal motion. (For interpretation of the references to color in this figure legend, the reader is referred to the web version of this article.)

Then, referring to particle advection scheme, 72×128 particles were put over each frame to simulate individuals of the shoal. Then the velocity and turning angle of each particle were estimated with the average optical flow of its 15×15 neighbor pixels in each frame. Finally, the particles with velocities greater than a changing threshold T (Eq. (3)) were regarded as the motion vectors of the shoal.

$$T = \sum_{i=1}^{72\times128} v_i / n_T \quad (3)$$

where n_T is the number of particles with velocities greater than zero in each frame.

2.3.2. Spatial behavioral characteristics, statistics and entropy-based dispersion measurement of the shoal

The dispersion of the shoal in each frame was calculated by projecting the motion vectors to m_1 bins of X-axis with m_{11} pixels wide and m_2 bins of Y-axis with m_{22} pixels wide simultaneously. Then, statistical joint histogram related to the motion vectors was considered in this section. h_{xy} denotes the number of motion vectors projected to X-axis at the m_1-th bin and Y-axis at the m_2-th bin in the meantime (Eq. (4)).

$$h_{xy}(i_1,j_1) = \{k_{xy}(i_1,\ j_1),\ 0 \leqslant i_1 \leqslant m_1,\ 0 \leqslant j_1 \leqslant m_2\};$$
$$p_{xy}(i_1,j_1) = (h_{xy}(i_1,\ j_1)/M) \times 100\% \quad (4)$$

In this section, m_{11} is set to 60, m_{22} is set to 30; m_1 and m_2 are equal to 32 and 36, respectively. M is the total number of the motion vectors in each frame. k_{xy} as well as h_{xy} denotes the statistical number of the motion vectors classified into the corresponding sections of the X- and Y-axis simultaneously, and p_{xy} is the probability of the corresponding k_{xy}.

Figs. 4 and 5 show the statistical joint histograms containing the dispersion information of the shoal. Horizontal direction represents X-axis, vertical direction represents Y-axis. The color bar with the unit % in this article is the expression of the occurrence probability of the motion vectors, different color represents different probability. As shown in Figs. 4 and 5, it is obvious that the higher degree of gathering of the shoal, the more occurrences of the high probability.

Entropy acts on the statistical features of the entire information source and is also the expression of the general characteristics of the information source in evaluative meaning. In statistical mechanics, the thermodynamic system and the information theory, entropy have been widely applied and made many remarkable achievements. In statistical mechanics, entropy is used to measure uncertainty, and the greater entropy means the higher disorder (Sethna, 2006). In a thermodynamic system, entropy is also usually related to the notions of disorder and chaos (Abe et al., 2001). In the information theory, entropy is also often taken to measure the uncertainty and disorder in a random variable (Biaynicki-Birula and Mycielski, 1975). In this section, in order to measure the dispersion level of shoal, the definition of combination entropy in information theory was referred as (Jiang et al., 2010):

$$CE = -\sum_{i_1}^{m_1}\sum_{j_1}^{m_2}(p_{xy}(i_1,j_1))\log_2(p_{xy}(i_1,j_1)) \quad (5)$$

To CE, a low entropy value means a gathering distribution contrasted to a relative scattering distribution.

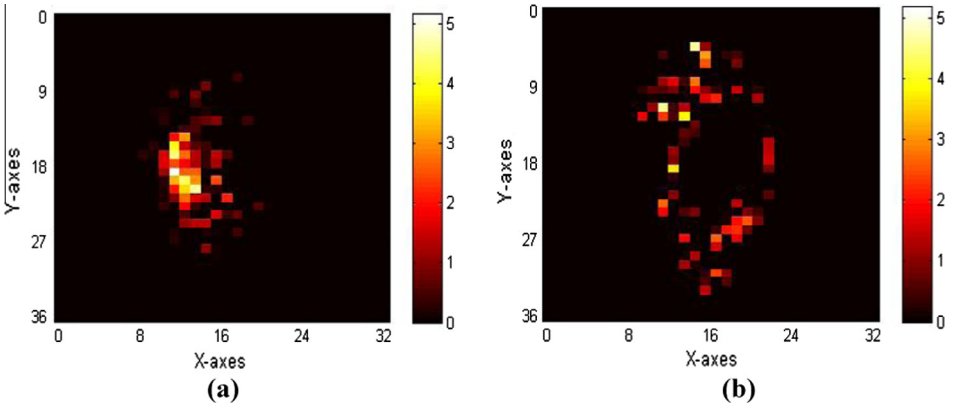

Fig. 4. BMFS based statistical joint histograms of the dispersion of the shoal: (a) gathering behavior, (b) scattering behavior.

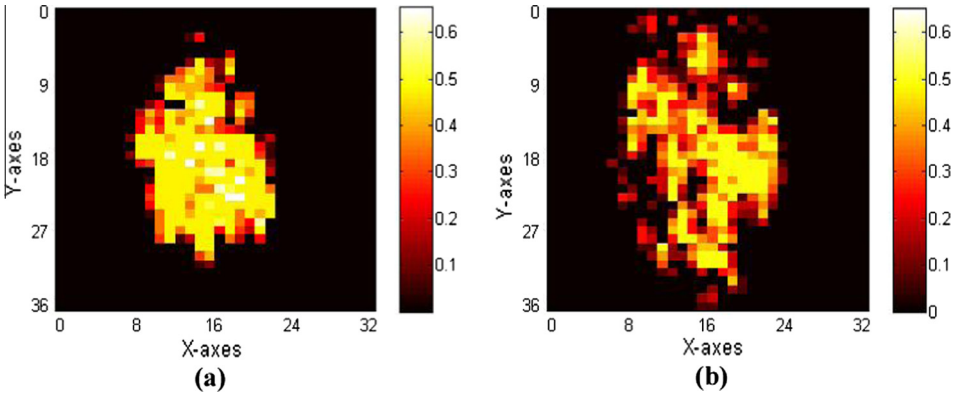

Fig. 5. PAOF based statistical joint histograms of the dispersion of the shoal: (a) gathering behavior, (b) scattering behavior.

2.3.3. Entropy-based changing magnitude measurement of the behavioral characteristics of the shoal

In this section, the velocity and turning angle obtained through the optical flow were regarded as the key factors. The processing procedure is shown below.

The consecutive three frames were marked as f_1, f_2 and f_3, respectively, and the optical flow $\boldsymbol{P}$, $\boldsymbol{Q}_1$ and $\boldsymbol{Q}_2$ were separately calculated between f_1 and f_3, f_1 and f_2, f_2 and f_3. Then, the velocity ($\boldsymbol{V}$) and turning angle (θ) of the consecutive three frames were obtained by means of Eqs. (6) and (7), respectively.

$$V = |P| \tag{6}$$

$$\theta = \arccos(Q_1 * Q_2 / |Q_1||Q_2|) \tag{7}$$

The scopes of the velocity and turning angle of motion vectors were divided into a number of sections in this study. Figs. 6 and 7 (based on BMFS and PAOF, respectively) are the statistics joint histograms of the velocity and turning angle. Vertical axis represents the velocity (*bl* is the body length of the fish (Xu et al., 2006), which is regarded as the speed unit), horizontal axis stands for the turning angle (Eq. (8)). To avoid high statistical dimension, the scopes of the velocity and turning angle were set to 0–1.0 *bl*/s and 0–180°, respectively, and the former was counted at intervals of 0.05 *bl*/s ($n_1 = 20$), and the latter was counted at intervals of 5° ($n_2 = 36$).

$$\begin{aligned} &h_{sa}(i_2, j_2) = \{k_{sa}(i_2, j_2),\ 0 \leqslant i_2 \leqslant n_1,\ 0 \leqslant j_2 \leqslant n_2\}; \\ &p_{sa}(i_2, j_2) = (h_{sa}(i_2, j_2))/M \times 100\% \end{aligned} \tag{8}$$

where k_{sa} as well as h_{sa} is the statistical number of the motion vectors classified into the corresponding sections of the speed and angle simultaneously, and p_{sa} is the probability of the corresponding k_{sa}.

Figs. 6 and 7 express similar phenomenon: the number of high occurrence probability in emergent behavior is less than that in normal behavior, but the occurrence probability of high velocity shows the contrary characteristic.

Then, similar to Eq. (5), the changing magnitude of the behavioral characteristics was measured as Eq. (9).

$$D = -\sum_{i_2}^{n_1}\sum_{j_2}^{n_2}(p_{sa}(i_2, j_2))\log_2(p_{sa}(i_2, j_2)) \tag{9}$$

To Eq. (9), the higher value of D, the more intense emergent behavior.

2.4. Modified kinetic energy model-based behavior measurement of the shoal

Based on the above analysis, a novel modified kinetic energy model combined with the dispersion information, velocity and turning angle of the shoal was defined as:

$$E_{(kn)} = \begin{cases} (D + 100)^2 \times (-CE) \rightarrow BMFS \\ (D + 100)^2 / (CE) \rightarrow PAOF \end{cases} \tag{10}$$

The value of modified kinetic energy model $E_{(kn)}$ would vary intensely when special behaviors of the shoal happen.

To validate the feasibility of KEM, with the help of MATLAB 2013a computing environment and human observation, special behaviors including emergent gathering and scattering caused by

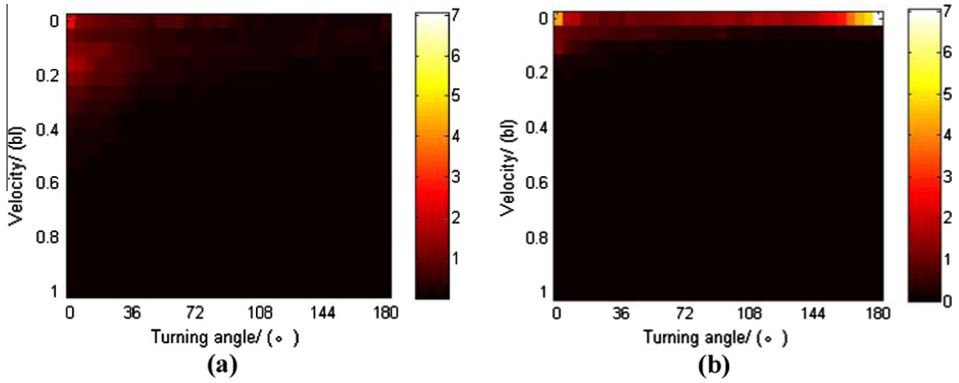

Fig. 6. BMFS based statistical joint histograms of the motion characteristics: (a) emergent behavior, (b) normal behavior.

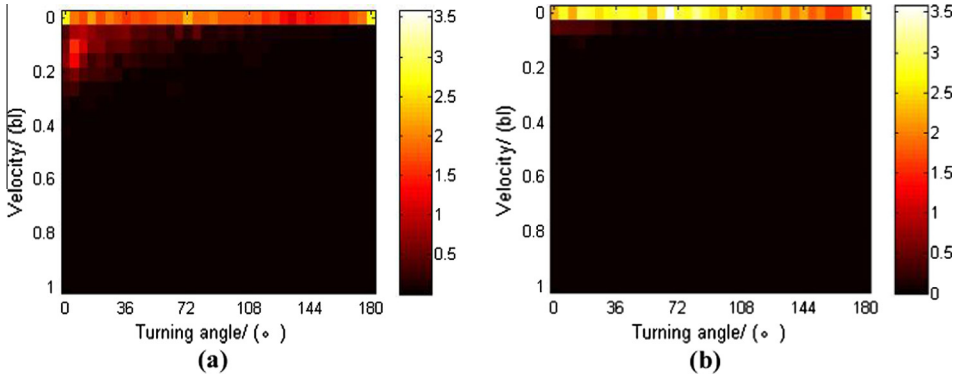

Fig. 7. PAOF based statistical joint histograms of the motion characteristics: (a) emergent behavior, (b) normal behavior.

some stimuli were used. For convenience, both p_{sa} and p_{xy} were multiplied by integer 100 in calculation of D, CE and $E_{(kn)}$.

3. Results

According to the comparisons of numerous optical flow methods (Barron et al., 1994), Lucas-Kanade optical flow (Lucas and Kanade, 1981) based on local difference method among a fixed number of frames is the best precise and reliable optical flow method due to the less computation and more flexible resulted from only few feature points should be tracked. What's more, Lucas-Kanade optical flow is also a method in which the optical flow in a small-spaced window can be regulated when the changes in the test image are assumed to be constant. Thus, Lucas-Kanade optical flow was adopted to calculate the optical flow of the shoal in this study.

Fig. 9 shows the dispersion measurement of the shoal in the test video (Fig. 8). The gathering behavior occurs before the black dotted line (frame order: 155 ± 2) set according to the human observation, and the scattering behavior happens immediately following the dotted line. The lower CE is, the more obvious gathering behavior the shoal would be. Due to the different extractive styles of the behavioral characteristics, the turning points of the curves about the watershed between the emergent gathering and scattering are not same but similar.

Fig. 10 is the representation of the changing magnitude of the behavioral characteristics of the shoal in the test video. As shown in Fig. 10, the curves change obviously when the emergent behaviors (frame orders: 68 ± 2 and 155 ± 2) occur. The greater D is, the more intense behavior the shoal would be.

The modified kinetic energy model based behavior measurement of the shoal was demonstrated as follows:

Contrasted to Figs. 9 and 10, Fig. 11 delivers to us more information of the special behavior, because of both the dispersion and changing magnitude of the behavioral characteristics were taken into account. Only when the requirements of the thresholds (blue solid line, determined by amounts of experiments) which were set in Fig. 9 (lower than the threshold), Fig. 10 (greater than the threshold) and Fig. 11 (greater than the threshold) all are met, the detection of the special behavior of the shoal would be confirmed. In the meantime, in order to obtain the stable results, only when the requirements mentioned above last for d consecutive frames do the system alarm and d was set to 10 in this study according to amounts of the experiments.

According to the evacuation of the gastro-intestine contents-based long experiment in RAS, the KEM-based detection results of the emergent gathering and scattering are revealed in Fig. 12 and Table 1. It should be noted that, to achieve the high accuracy rate of the detection, thresholds in Figs. 9–11 were determined independently. As a consequence, the rise of the missing report rate would result in.

In Fig. 12, the time of duration (36 h) of the evacuation experiment is divided into ten periods in order, i.e., each period contains 3.6 h. As shown in Fig. 12(a), although the difference of the average accuracy rate between BMFS (blue) and PAOF (red) in each period is not obvious, the opposite phenomenon is performed in Fig. 12 (b). Similar information also can be obtained from Table 1. In particular, the distribution character of bar chart of PAOF as well as BMFS in Fig. 12(b) is subordinate to the approximately normal distribution to some extent.

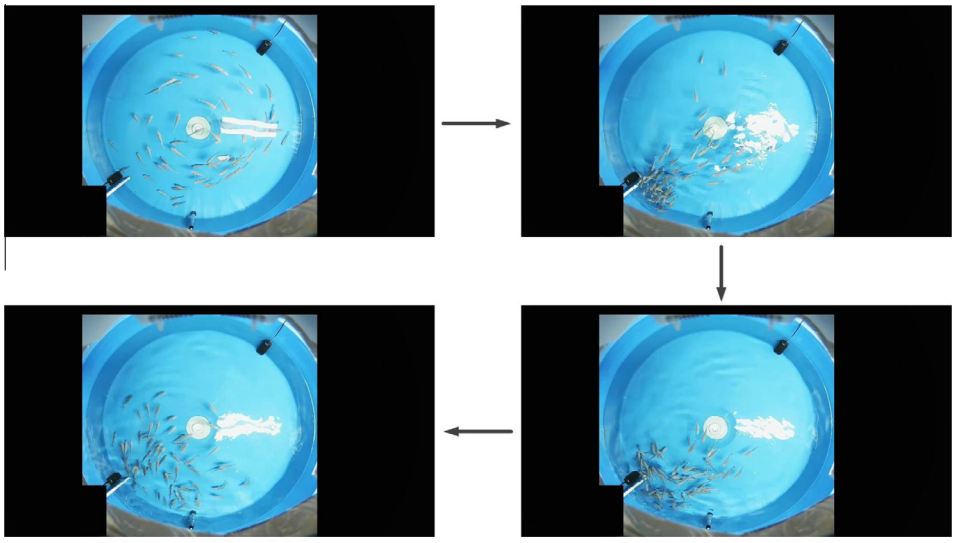

Fig. 8. The moving trend of the shoal in the test video.

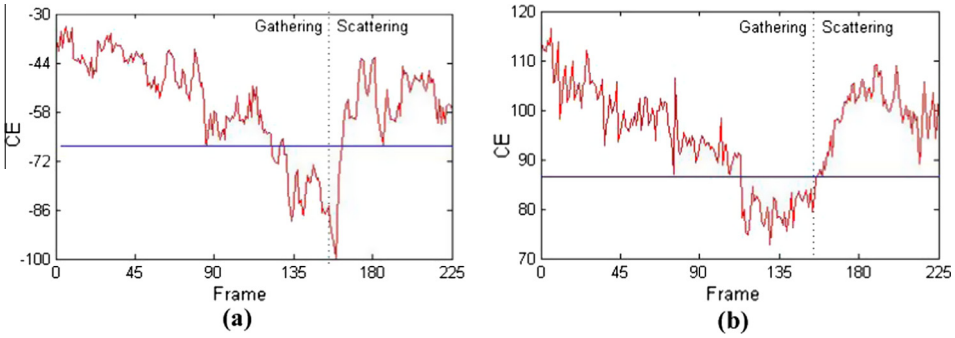

Fig. 9. (a) BMFS based dispersion measurement of the shoal, (b) PAOF based dispersion measurement of the shoal.

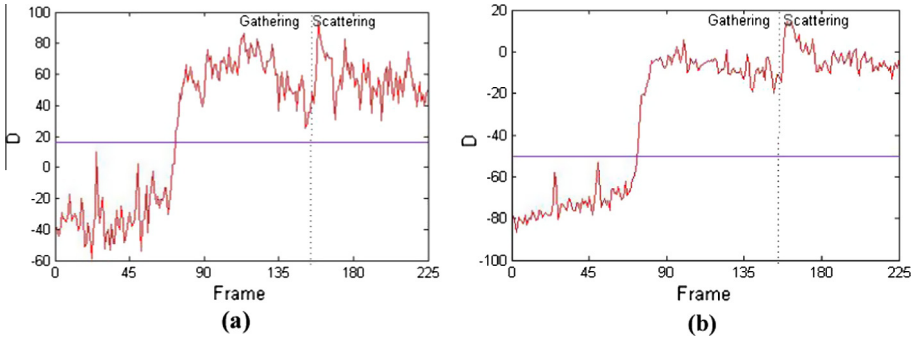

Fig. 10. (a) BMFS based changing magnitude of the behavioral characteristics of the shoal, (b) PAOF based changing magnitude of the behavioral characteristics of the shoal.

4. Discussion

In general, as described in Fig. 12 and Table 1, due to the relatively stable foreground segmentation, BMFS-based KEM shows better performance in detection of special behaviors of the shoal. Although PAOF-based KEM also shows relatively good accuracy rate, it is at the cost of the higher missing report rate. The reasons of this phenomenon may be:

1. Improper determination of the velocity threshold (Eq. (3))—quite a number of the particles were influenced by the fluctuation of the water surface especially when the intense emergent behavior happened (as a solution, a self-adaptive square error analyzing method (Ostu, 1979) may provide a good reference to optimize the determination of the velocity threshold); and/or
2. Removing of the reflective regions—the removed regions may contain important behavioral characteristics of the shoal. As a solution, the appropriate interpolation processing (Sarfraz, 2000) of the reflective regions combined with polarising filter (Hiramoto et al., 2010) may show better performance, in contrast to direct removal.

Nevertheless, PAOF-based KEM may show a better prospect in industrial RAS because the foreground segmentation is not needed. It should be mentioned that, as to BMFS-based KEM, because of the

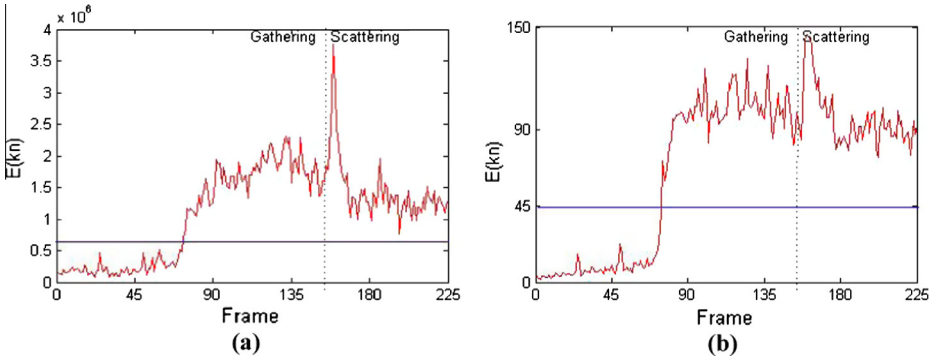

Fig. 11. (a) BMFS and modified kinetic energy model based behavior measurement of the shoal, (b) PAOF and modified kinetic energy model based behavior measurement of the shoal.

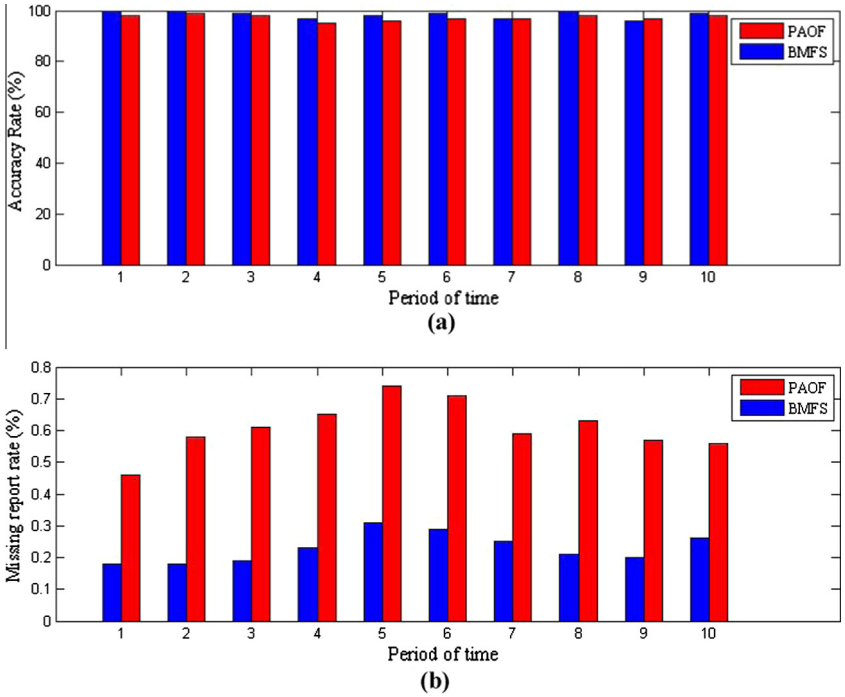

Fig. 12. (a) Average accuracy rate of KEM based detection of special behaviors, (b) average missing report rate of KEM based detection of special behaviors.

Table 1
KEM based detection results of special behaviors based on Fig. 12.

Detection method	Average accuracy rate (%)	Average missing report rate (%)
BMFS based KEM	98.41 ± 1.33[a]	0.23 ± 0.05[a]
PAOF based KEM	97.20 ± 1.23[a]	0.61 ± 0.08[b]

[a-b] Different lowercase letters in the same column are significantly different ($p < 0.05$).

white color of the water outlet (in the middle of the rearing tank), intensity of the signal in Cr component is similar to that of fish in Cr component. Thus, fish in this area would be hard to detect. This problem, however, can be avoided by making the outlet blue in color which is similar to the background color of the tank.

In addition, although an improved average background modeling based foreground segmentation was proposed, disturbance of the reflection still existed. As a consequence, the reflection noise may be detected as a fish sometimes. Therefore, proper processing of the reflective regions, as mentioned above, is necessary.

Specifically, phenomenon of the approximately normal distributions of the bar charts in Fig. 12(b) might be caused by the changing physiological property of the shoal, which underwent the evacuation of the gastro-intestine contents. In the first half of the shoal's evacuation of the gastro-intestine contents, the hunger level of the shoal exacerbated as time went on. As a consequence, shoal's behaviors as well as the reflection of the water surface became intense (Wyatt, 1972). Then, the missing report rate was affected and showed an upward trend. However, in the second half of the shoal's evacuation, a downward trend of the missing report rate was presented. The sharp consumption of the blood glucose of the shoal may be the crucial point (Olmeda et al., 2009). Therefore, to conserve energy, the shoal may regulate its motion strategy and make the motion slow down (Miller et al., 2013; Couzin et al., 2005).

Despite all these, some challenges of KEM still exist. For example, the body length of the fish should be measured at regular intervals due to the standardization of the velocity in this study. Whereas, most works on fish length measurement were in laboratory-scale (Beddow et al., 1996; Petrell et al., 1997; Costa

et al., 2006). Relevant practical and automatic measuring methods, which are suitable for real industrial RAS, haven't been reported. In addition, the experiment in this study was conducted in a laboratory-controlled RAS, where the shoal was easily distinguished from the background due to the contrast between the dark-blue background and the gray skin of the tilapia. However, many studies have shown that tilapia (Xu et al., 2006), as well as many other fish species, can change their skin color to adapt to ambient color (Hiroshi et al., 1989; Fujimoto et al., 1991; Papoutsoglou et al., 2000).

In view of problems mentioned above, the research focused on real-time, economical and practical measurement of fish length, as well as the detection of the cultured targets from backgrounds in industrial RAS with a complex aquaculture environment, should be attached importance to. Actually, as to the challenges mentioned above, nutrition, physiology and ethology-based solutions may be possible. To the first challenge, "Fish-PrFEQ" (Cho and Bureau, 1998; Zhou et al., 2005), as a practical bioenergetics model in fish and shrimp farming, has a good performance in predicting the growing states, nutrition supply and feed conversion of the cultured objects. Thus, by means of "Fish-PrFEQ", the rough estimation of the body length of the fish may be possible. As to the second challenge, spectrum-based means are recommendable. According to Volpato et al. (2013) and Luchiari and Pirhonen (2008), different fish have different preference for the ambient color and the growth of the fish is also influenced deeply by the rearing environmental color. Thus, in the condition of the certain background color of the rearing tank, the proper color-based lighting may be conductive to distinguish fish from the background by camera, such as the green lighting which is combined with the blue background of rearing tank for juvenile rainbow trout (Luchiari and Pirhonen, 2008).

In this paper the main purpose of this research was the verification of the feasibility of KEM. As a consequence, determination of the corresponding shoal behaviors, namely velocities, turning angles, *X*-axis and *Y*-axis partitions, were not considered.

5. Conclusions

For fish welfare, a non-invasive and effective method aimed at detecting special behaviors of the shoal in RAS was proposed in this article. In consideration of the dispersion, velocity and turning angle of the shoal, a novel modified kinetic energy model was presented. Then, through the evacuation of the gastro-intestine contents-based experiment, the feasibility of KEM was validated due to the good performance in detection of special behaviors. Although BMFS-based KEM performs better statistically, PAOF-based KEM shows the higher practical value. This research aims to provide reliable theoretical supports for real-time smart supervision system in RAS. Due to the application of the optical flow, complex tracking of individual fish was avoided. Furthermore, because of the processing of the reflective regions of the water surface and the standardization of the behavioral characteristics, method developed in this study shows reliable robustness to the proper fluctuation of the water surface (which is caused by the motion of the shoal) as well as the changing density of the shoal.

Acknowledgements

This research was supported by the Project of the National "Twelfth Five-Year" Plan for Science & Technology (Grant No. 2014BAD08B09), ZHEJIANG Province Key R&D Project (2015C02010) and the National Natural Science Foundation of China (No. 31402352). Any opinions, findings, and conclusions expressed in this publication are those of the authors and do not necessarily reflect the views of Zhejiang University.

References

Abe, S., Martnez, S., Pennini, F., Plastino, A., 2001. Nonextensive thermodynamic relations. Phys. Lett. A 281 (2), 126–130.
Ali, S., Shah, M., 2007. A Lagrangian particle dynamics approach for crowd flow segmentation and stability analysis. In: IEEE Conference on Computer Vision and Pattern Recognition (CVPR), Minneapolis, MN, pp. 1–6.
Amundsen, P., Klemetsen, A., 1988. Diet, gastric evacuation rates and food consumption in a stunted population of *Arctic charr*, *Salvelinus alpinus* L., in Takvatn, northern Norway. J. Fish Biol. 33 (5), 697–709.
Barron, J.L., Fleet, D.J., Beauchemin, S.S., 1994. Performance of optical flow techniques. Int. J. Comput. Vis. 12 (1), 43–77.
Beddow, T.A., Ros, L.G., Marchant, J.A., 1996. Predicting salmon biomass remotely using a digital stereo-imaging technique. Aquaculture 146, 189–203.
Biaynicki-Birula, I., Mycielski, J., 1975. Uncertainty relations for information entropy in wave mechanics. Commun. Math. Phys. 44 (2), 129–132.
Campenhausen, C.V., Riess, L., Weissert, R., 1981. Detection of stationary objects by the blind cave fish *Atwptichthys jordani* (*Characidae*). J. Comp. Physiol. A 143 (3), 369–374.
Cao, T., Wu, X.Y., Guo, J.N., Yu, S.Q., Xu, Y.S., 2009. Abnormal crowd motion analysis. In: Proceedings of the 2009 IEEE International Conference on Robotics and Biomimetics, Guilin, China, pp. 1709–1714.
Cho, C.Y., Bureau, D.P., 1998. Development of bioenergetics models and the Fish-PrFEQ software to estimate production, feeding ration and waste output in aquaculture. Aquat. Living Resour. 11, 199–210.
Conrad, J.L., Weinersmith, K.L., Brodin, T., Saltz, J.B., Sih, A., 2011. Behavioural syndromes in fishes: a review with implications for ecology and fisheries management. J. Fish Biol. 78, 395–435.
Couzin, I.D., Krause, J., Franks, N.R., Levin, S.A., 2005. Effective leadership and decision-making in animal groups on the move. Nature 433 (7025), 513–516.
Costa, C., Loy, A., Cataudella, S., Davis, D., Scardi, M., 2006. Extracting fish size using dual underwater cameras. Aquacult. Eng. 35, 218–227.
Dalsgaard, J., Lund, I., Thorarinsdottir, R., Drengstig, A., Arvonen, K., Pedersen, P.B., 2013. Farming different species in RAS in Nordic countries: current status and future perspectives. Aquacult. Eng. 53, 2–13.
Delcourt, J., Becco, C., Vandewalle, N., Poncin, P., 2009. A video multitracking system for quantification of individual behavior in a large fish shoal: advantages and limits. Behav. Res. Methods 41 (1), 228–235.
Delcourt, J., Denoel, M., Ylieff, M., Poncin, P., 2013. Video multi-tracking of fish behavior: a synthesis and future. Fish Fish. 14, 186–204.
Fujimoto, M., Arimoto, T., Morishita, F., Naitoh, T., 1991. The background adaptation of the *flatfish*, *Paralichthys olivaceus*. Physiol. Behav. 50, 185–188.
Gonzalez, R.C., Woods, R.E., 2002. Digital Image Processing, second ed. Prentice Hall, New Jersey.
Gui, F., Li, Y., Dong, G., Guan, C., 2006. Application of CCD image scanning to sea-cage motion response analysis. Aquacult. Eng. 35, 179–190.
Guo, G.X., Jun, C., Xin, Y.W., Yen, L.C., Yong, S.O., Yang, S.X., 2012. An energy model approach to people counting for abnormal crowd behavior detection. Neurocomputing 83, 121–135.
Hiramoto, K., Yamate, Y., Orita, K., Jikumaru, M., Kasahara, E., Sato, E.F., Tamura, S., Inoue, M., 2010. Prevention of scattered light-induced asthenopia and fatigue by a polarized filter. Photodermatol. Photoimmunol. Photomed. 26 (2), 89–92.
Hiroshi, N., Haruhisa, N., Ryozo, F., Noriko, O., 1989. Correlation between bodycolor and behavior in the upside-down *catfish*, *Synodontis nigriventris*. Comp. Biochem. Physiol. Part A. Physiol. 92, 323–326.
Israeli, D., Kimmel, E., 1996. Monitoring the behavior of hypoxia stressed *Carassius auratus* using computer vision. Aquacult. Eng. 15, 423–440.
Jiang, A.H., Huang, X.C., Zhang, Z.H., Li, J., Zhang, Z.Y., Hua, H.X., 2010. Mutual information algorithms. Mech. Syst. Signal Process. 24, 2947–2960.
Jones, R.C., 2013. Science, sentience, and animal welfare. Biol.-Philos. 28 (1), 1–30.
Kane, A.S., Salierno, J.D., Gipson, G.T., Molteno, T.C.A., Hunter, C., 2004. A video-based movement analysis system to quantify behavioral stress responses of fish. Water Res. 38, 3993–4001.
Kiessling, A., Van, D.V.H., Flik, G., 2012. Welfare of farmed fish in present and future production system. Fish Physiol. Biochem. 38 (1), 1–3.
Le François, N.R., Jobling, M., Carter, C., Blier, P., 2010. Finfish Aquaculture Diversification. Cabi, Cambridge.
Liu, Z.Y., Lia, X., Fan, L.Z., Lu, H.D., Liu, L., Liu, Y., 2014. Measuring feeding activity of fish in RAS using computer vision. Aquacult. Eng. 60, 20–27.
Lucas, B.D., Kanade, T., 1981. An iterative image registration technique with an application to stereo vision. In: Proceedings of Imaging Understanding Workshop, Vancouver, British Columbia, pp. 121–130.
Luchiari, A.C., Pirhonen, J., 2008. Effects of ambient colour on colour preference and growth of juvenile rainbow trout *Oncorhynchus mykiss* (Walbaum). J. Fish Biol. 72 (6), 1504–1514.
Mancera, J.M., Vargas-Chacoff, L., Garcia-Lopez, A., Kleszczynska, A., Kalamarz, H., Martinez-Rodriguez, G., Kulczykowska, E., 2008. High density and food deprivation affect arginine vasotocin, isotocin and melatonin in *gilthead sea bream* (*Sparus auratus*). Comp. Biochem. Physiol. A 149, 92–97.
Masud, S., Singh, I.J., Ram, R.N., 2005. Behavioural and hematological responses of *Cyprinus carpio* exposed to mercurial chloride. J. Environ. Biol. 26, 393–397.

Miller, N., Gerlai, R., 2007. Quantification of shoaling behaviour in *zebrafish* (*Danio rerio*). Behav. Brain Res. 184, 157–166.
Miller, N., Gerlai, R., Hartnett, A.T., Couzin, I.D., 2013. Both information and social cohesion determine collective decisions in animal groups. PNAS 110 (13), 5263–5268.
Olmeda, J.F.L., Álvarez, M.E., Vázquez, F.J.S., 2009. Glucose tolerance in fish: Is the daily feeding time important? Physiol. Behav. 96 (4–5), 631–636.
Ostu, N., 1979. A threshold selection method from gray-level histogram. IEEE Trans. Syst. Man Cybern. 9 (1), 62–66.
Papadakis, V.M., Papadakisa, I.E., Lamprianidou, F., Glaropoulos, A., Kentouri, M., 2012. A computer-vision system and methodology for the analysis of fish behavior. Aquacult. Eng. 46, 53–59.
Papoutsoglou, S., Mylonakis, G., Miliou, H., Karakatsouli, N., Chadio, S., 2000. Effects of background color on growth performances and physiological responses of *scaled carp* (*Cyprinus carpio* L.) reared in a closed circulated system. Aquacult. Eng. 22, 309–318.
Petrell, R.J., Shi, X., Ward, R.K., Naiberg, A., Savage, C.R., 1997. Determining fish size and swimming speed in cages and tanks using simple video techniques. Aquacult. Eng. 16, 63–84.
Polten, B., 2007. Status of law-making on animal welfare. Deutsche Tierarztliche Wochenschrift 114 (3), 98–103.
Pratt, T.C., Smokorowski, K.E., Muirhead, J.R., 2005. Development and experimental assessment of an underwater video technique for assessing fish-habitat relationships. Arch. Hydrobiol. 164, 547–571.
Robbert, C., 2009. Automated analysis of behavior in *zebrafish larvae*. Behav. Brain Res. 203, 127–136.
Sarfraz, M., 2000. A rational cubic spline for the visualization of monotonic data. Comput. Graph. 24, 509–516.
Sethna, J.P., 2006. Statistical Mechanics: Entropy, Order Parameters, and Complexity. Oxford University Press, New York.
Sobel, I., 1990. An isotropic 3×3 image gradient operator. In: Freeman, H. (Ed.), Machine Vision for Three-dimensional Sciences. Academic Press, New York, pp. 376–379.
Stien, L.H., Brafland, S., Austevollb, I., Oppedala, F., Kristiansen, T.S., 2007. A video analysis procedure for assessing vertical fish distribution in aquaculture tanks. Aquacult. Eng. 37, 115–124.
Tang, G.Y., 1982. A discrete version of Green's theorem. IEEE Trans. Pattern Anal. 4 (3), 242–249.
Vassilis, M.P., Ioannis, E.P., Fani, L., Alexios, G., Maroudio, K., 2012. A computer-vision system and methodology for the analysis of fish behavior. Aquacult. Eng. 46, 53–59.
Vogl, C., Grillitsch, B., Wytek, R., Spieser, O.H., Scholz, W., 1999. Qualification of spontaneous undirected locomotor behavior of fish for sublethal toxicity testing. Part I. Variability of measurement parameters under general test conditions. Environ. Toxicol. Chem. 18, 2736–2742.
Volpato, G.L., Bovi, T.S., Freitas, H.A., Silva, D.F., Delicio, H.C., Giaquinto, P.C., Barreto, R.E., 2013. Red light stimulates feeding motivation in fish but does not improve growth. PLoS ONE 8 (3), 1–5.
Wyatt, T., 1972. Some effects of food density on the growth and behavior of *plaice larvae*. Mar. Biol. 14 (3), 210–216.
Xu, J.Y., Liu, Y., Cui, S.R., Miao, X.W., 2006. Behavioral responses of tilapia (*Oreochromis niloticus*) to acute fluctuations in dissolved oxygen levels as monitored by computer vision. Aquacult. Eng. 35, 207–217.
Zhong, Z., Ye, W., Wang, S., Yang, M., Xu, Y., 2007. Crowd energy and feature analysis. In: IEEE International Conference on Integration Technology, Shenzhen, China, pp. 144–150.
Zhou, A., Xie, S., Lei, W., Zhu, X., Yang, Y., 2005. A bioenergetics model to estimate feed requirement of gibel carp, *Carassius auratus gibelio*. Aquaculture 248 (1), 287–297.